ORIGINAL ARTICLE

A Quality by Design Paradigm for Albumin-Based Nanoparticles: Formulation Optimization and Enhancement of the Antitumor Activity

Marwa H. S. Dawoud[1,4] · Amira Abdel-Daim[2] · Mai S. Nour[3] · Nabila M. Sweed[1]

Abstract

Purpose Albumin nanoparticles are promising carriers for therapeutic agents, owing to their biocompatibility, safety, and versatility in fabrication. The formulation of albumin nanoparticles is highly affected by many product and process variables, resulting in a great variation in these nanoparticles. The aim of this work was to formulate and optimize albumin nanoparticles loaded with silymarin, as a model drug with low bioavailability, for the treatment of hepatocellular carcinoma, using quality by design (QbD) approach.

Methods A thorough risk assessment for albumin nanoparticles formulation was developed and a complete quality product profile was defined using the QbD approach. A D-optimal design was used to optimize the amount of albumin and drug, which significantly affected the particle size (PS) and the entrapment efficiency (EE%), which was further tested on hepatocellular carcinoma.

Results A design space was constructed, with an optimized formula showing a PS of 135 nm, a polydispersity index (PDI) of 0.09, an EE% of 88%, and a zeta potential of -12.5 mV. The optimized formula (O_1) with spherical particles, showed an extended-release rate as compared to free silymarin. Moreover, a pronounced anti-proliferation activity of O_1 was observed on human hepatocellular carcinoma cell line HepG2 than the free drug. The flow cytometric analysis of the cell cycle showed a significant suppression of the S-phase after treating the HepG2 cell with O_1, but not with free silymarin.

Conclusion Thus, a detailed QbD study has been conducted, with deep product and process understanding, and resulted in a successful formulation of silymarin albumin nanoparticles for the suppression of hepatocellular carcinoma.

Keywords Risk assessment · D-Optimal design · Hepatocellular carcinoma · Quality Target Product Profile · Optimization

Introduction

Nano-drug delivery systems have recently gained much attention in the site-specific delivery of various drugs, as well as in disease management. Their versatile nature allowed them to incorporate poorly soluble drugs, leading to an increase in the bioavailability of many drugs that were previously not administered orally [1]. Nanoparticles prepared using non-biodegradable polymers could not be considered for systemic use [2]; and thus, efforts have been made to use biodegradable polymers to reduce the side effects, and allow for the systemic use of such systems [3]. This, in turn, leads to the use of nanoparticles in the treatment of many fatal diseases such as cancer, cardiovascular diseases, AIDS, and intracellular infections [4, 5].

Great focus has been made on the use of albumin in the preparation of nanoparticles for the treatment of many diseases [6], owing to its biocompatibility and biodegradability [7, 8].

Albumin is an abundant protein representing about 52–62% of the total plasma proteins. It has a major role in the transport of many compounds such as fatty acids, metals, amino acids, and therapeutic drugs [9]. Furthermore,

✉ Marwa H. S. Dawoud
mdawoud@msa.edu.eg; marwa.hamdy@yahoo.com

[1] Department of Pharmaceutics, Faculty of Pharmacy, October University for Modern Sciences and Arts, Giza, Egypt

[2] Department of Biochemistry, Faculty of Pharmacy, October University for Modern Sciences and Arts, Giza, Egypt

[3] Department of Pharmaceutical Chemistry, Faculty of Pharmacy, October University for Modern Sciences and Arts, Giza, Egypt

[4] October University for Modern Sciences and Arts, Intersection of 26Th of July Road and Elwahat Road, 6Th of October City, Giza, Egypt

serum albumin is well known for its high ligand binding capacity, as it contains 11 binding sites for hydrophobic compounds [10]. Albumin nanoparticles could deliver drugs in a controlled and site-specific manner, thus minimizing their possible side effects [11]. Moreover, albumin possesses potential advantages over other synthetic polymers, as it has a high adsorption capacity, a high loading efficiency, and high stability in the blood. Thus, albumin can be used for the loading of many drugs to target their accumulation in the certain cells, as targeting anticancer drugs in the tumor cells. Albumin nanoparticles can be used for the incorporation of hydrophilic and hydrophobic compounds, owing to their subdomain IIA and IIIA, in addition to subdomain IB, that allows for the incorporation of hydrophobic drugs, complex heterocyclic drugs, and endogenous ligands [9, 12]. Bovine serum albumin (BSA) potentially binds drugs with a non-covalent bond, and it has a structure similar to that of the human serum albumin, except for the number of tryptophans [13].

Encapsulation of drugs into nanocarrier systems in order to achieve targeted drug delivery is promising, but faces many challenges to achieve it in the desired manner [14, 15]. Accordingly, a detailed and risk-based study of the whole process of preparation and optimization is needed to achieve the required target. Quality by design (QbD) is a strategic approach for product development, initiated by the Food and Drug Administration (FDA) [16]. It considers both product and process understanding, as well as the relationship between the critical process parameters (CPP), the material attributes (CMA), and the critical quality attributes (CQA), in order to establish a controlled design space [17]. This would result in a robust, and a high-quality product, which in turn would reduce the overall waste produced during manufacturing. QbD would also encourage more pharmaceutical companies and researchers across the world to adopt it [18]. Hence, the QbD approach, which assesses product and process understanding to achieve the desired product, allows for achieving a higher quality product [19].

The International Conference on Harmonization (ICH, Q8) describes QbD as a comprehensive and deep understanding of both the product and the process, as it covers the whole steps involved in the pharmaceutical process development [20].

Cancer is a leading cause of death worldwide, and it is predicted that by year 2030, there would be 12 million cancer deaths [2]. Several approaches have been adopted for cancer therapy, including chemotherapy, radiation therapy, gene therapy, surgical interference for removal of tumor cells, and photodynamic therapy. Chemotherapy is the most widely used; however, it has several limitations, owing to its toxicity on the normal cells. Several approaches have been considered to overcome this problem [21]. Targeted site-specific delivery of therapeutic compounds using albumin nanoparticles loaded with natural products is one of the approaches used to minimize the side effects on the normal cells [22–24]

Silymarin, one of the natural products, is a lipophilic extract from the seeds of the milk thistle plant, *Silybum marianum*, and has been widely used as a hepatoprotective drug. It has powerful antioxidant effects, as it reduces free radical production and lipid peroxidation. It also inhibits binding of toxins to the liver cell membrane, thus acting as a toxin blockade agent. Silymarin was found to protect from liver injury caused by several intoxicants in animal models, as well as in humans. Several studies have suggested that silymarin possesses potential anticancer activity against many types of cancers, such as liver and prostate cancers. Despite its potential therapeutic effects against several diseases, its use has been greatly restricted, owing to its low oral bioavailability (20–50%) [25]. The low oral bioavailability might be attributed to its low aqueous solubility, its high first pass effect, its low intestinal permeability, and its rapid excretion in bile and urine [26]. Several approaches have been used to overcome such problems, such as solid dispersions [27], which increased the solubility of silymarin by 23-fold [28], but solid dispersions are well known for their great instability [29]; and solid lipid nanoparticles [30], which enhanced the therapeutic effectiveness of silyamrin to prevent D-GaIN/TNF-α–induced liver damage [31] but are being characterized by their low loading efficiencies owing to their rigid structures [32]; self-nano-emulsifying drug delivery systems [33], which greatly enhanced the bioavailability of silymarin [34], but these systems are characterized by their poor palatability owing to their lipidic content [35]; and β-cyclodextrin [36], to enhance its solubility and overcome such problems.

The present study aims to formulate and optimize silymarin albumin nanoparticles by the use of QbD approach, to try as much as possible to overcome all the aforementioned drawbacks of the other systems for targeting and treating hepatocellular carcinoma, and to prepare a comprehensive quality product profile that could be used for many other albumin nanoparticle-based formulations.

Materials and Methods

Materials

Bovine serum albumin (BSA) was purchased from Caisson Labs (East, Smithfield, UT, USA). Sodium chloride was obtained from Merck (Darmstadt, Germany), while glutaraldehyde was purchased from Sigma Aldrich (St. Louis, MO), and isopropyl myristate from Lobachemie (Mumbai, India). Ethanol was obtained from Piochem (Giza, Egypt). Silymarin was a generous gift from Sedico Company (Giza, Egypt).

All materials and solvents were of analytical grade, and were used as purchased, from ADWIC Company (Giza, Egypt). HepG2 hepatocellular carcinoma cell line was obtained from Nawah Scientific Inc. (Mokatam, Cairo, Egypt). Cells were maintained in DMEM supplemented with 100 mg/mL of streptomycin, 100 units/mL of penicillin, and 10% of heat-inactivated fetal bovine serum in humidified, 5% (v/v) CO_2 atmosphere at 37 °C.

Methods

Fabrication of Albumin Nanoparticles

Desolvation technique was used for the preparation of albumin nanoparticles [37]. An appropriate amount of bovine serum albumin was accurately weighed and dissolved in distilled water or 10 mM sodium chloride solution in water. The pH of this solution was adjusted to 8 or 9 using 0.1 N sodium hydroxide solution. A magnetic stirrer (MMS-3000, Biosan LTD, UK) at 500 rpm at room temperature was used to prepare silymarin-loaded nanoparticles. First, silymarin was dissolved in ethanol (the desolvating agent), and then was continuously added to the previously prepared solution at a rate of 1 mL/min. Blank formula was prepared using the same procedure as above except for not adding silymarin [8]. After the addition of ethanol, cross-linking of the nanoparticles was induced by adding 8% glutaraldehyde solution in distilled water. The cross-linking process was continued by stirring for the specified period of time. The nanoparticles were further purified by the complete removal of ethanol using vacuum evaporation (Heidolph 2, Schwabach, Germany), followed by re-dispersion of the pellets in the same volume of distilled water or 10 mM solution of NaCl in water solution.

Molecular Docking

Docking was performed using MOE version 2014.0901. Silymarin was docked in the active site of bovine serum albumin obtained from the protein databank (www.rcsb.org) as a co-crystal structure in complex with 3,5-diiodosalicylic acid as native ligand (PDB ID: 4JK4). Prior to performing the docking protocol, protein–ligand complex obtained from the protein databank was subjected to 3D protonation, partial charges were calculated using Amber99 forcefield, water of crystallization was deleted, and the active site was isolated. Moreover, recognition of the active sites of amino acid was done where studying of the interaction between the active site amino acids and the ligand was accomplished. Validation was performed by re-docking of the native ligand and rmsd value of 0.478342503 was obtained as depicted in Fig. 1a.

The 3D structure of silymarin was built using MOE builder and was 3D protonated, subjected to conformation analysis using systematic search, and the least energetic conformer was selected and used for molecular docking.

Alpha triangle placement method was used for docking, without changing the default parameters. Poses were prioritized based on affinity London dG scoring method, and those with the best affinity were used for study of ligand receptor interactions.

Physicochemical Characterization

- Particle size, polydispersity index, and zeta potential

Photon correlation spectroscopy was used to measure the particle size (in terms of hydrodynamic diameters), particle size distribution (in terms of polydispersity index (PDI)), and zeta potential (z-pot) using zetasizer (Malven Zetasizer version 6.20 serial number: MAL 104 4595, Worcestershire, UK). The scattering angle was adjusted to 90° at a temperature of 25 °C, after suitable dilutions. Disposable polystyrene cuvettes were used for the PS and PDI determination, whereas fixed glass cell was used for the z-pot determination [38]. Triplicate samples were used throughout the whole study.

- Morphological determination using transmission electron microscopy

Morphological examination of albumin nanoparticles was analyzed using transmission electron microscopy (TEM) (Joel JEM-1400, Tokyo, Japan). The samples were properly diluted with distilled water, then were added to a carbon film-covered grid that was negatively stained with phosphotungistic acid. The grid with the sample was dried and observed with TEM [39].

Determination of Entrapment Efficiency Percentage (EE%) and Percentage Yield (% yield)

Separation of the un-entrapped silymarin from the entrapped drug was accomplished by centrifugation at $14,000 \times g$ (Megafuge 16R, Hanau, Germany) at 4 °C for 30 min, followed by washing of the precipitate twice with distilled water. The un-entrapped drug in the supernatant was measured spectrophotometrically, after filtration through a 0.22-µm Millipore® filter, and suitable dilution. At a predetermined wavelength, $\lambda max = 286$ nm, the absorbance was measured, and the entrapment efficiency was calculated as follows [9]:
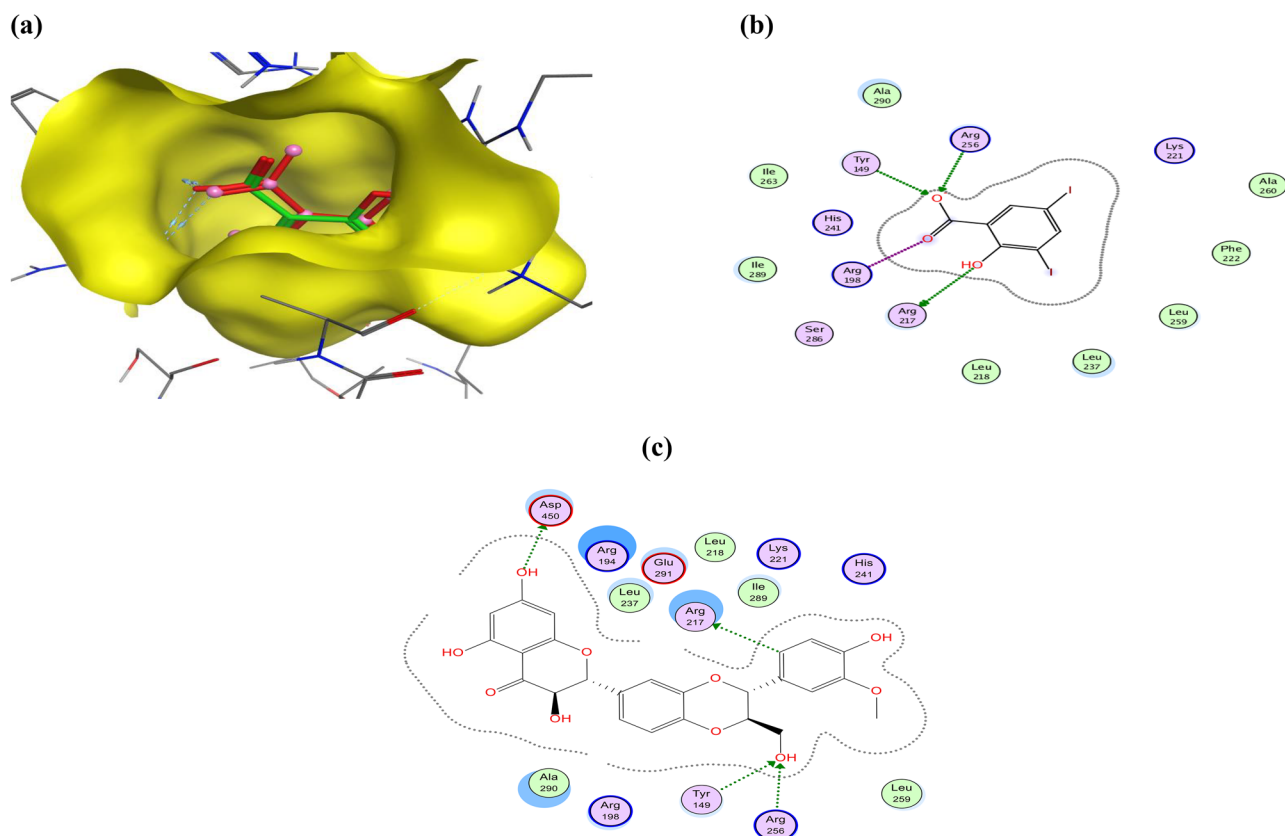
(a)

(b)

(c)

Fig. 1 **a** 3D overlay of the native (green) and re-docked ligand (red), **b** 2D interactions of native ligand, **c** 2D interactions of silymarin with bovine serum albumin

$$Silymarin\ EE\% = \left(1 - \frac{amount\ of\ free\ drug\ in\ supernatant}{amount\ of\ drug\ added}\right) * 100 \tag{1}$$

The percentage yield and the drug loading %, calculated using Eqs. 2 and 3, were measured after washing the precipitate and then it was dried and weighed [9, 40]:

$$Percentage\ yield = \left(\frac{weight\ of\ the\ nanoparticles}{Albumin + Drugamount}\right) * 100 \tag{2}$$

$$Drug\ loading\% = \left(\frac{amount\ of\ drug\ in\ nanoparticles}{Albumin + Drugamount}\right) * 100 \tag{3}$$

In Vitro Release Study

Dialysis bag method was used to test the in vitro release of both silymarin from albumin nanoparticles, and the corresponding silymarin standard dispersion in water. Briefly, silymarin albumin nanoparticles corresponding to 3 mg silymarin (optimized formula), or 3 mg silymarin in 10 mM solution of NaCl in water (standard), were placed in cellulose

dialysis bags (cutoff 12,000–14,000 Da) (Spectrum Medical Inc.,Los Angeles, CA, USA), which were immersed in 100 mL phosphate buffer saline (PBS) with pH 7.4 at 37 °C, under constant shaking (incubator shaker, ZHWY-2102C, Shanghai, China), at 100 rpm. The dialysis bags, presoaked in PBS, were firmly clipped from both ends before being immersed in the release medium. Three-milliliter samples were withdrawn at 0, 0.5, 1, 2, 3, 4, 5, 6, 8, 12, and 24 h, and were replaced with fresh buffer to maintain sink conditions. The samples were measured spectrophotometrically to determine the concentration of each sample [41]. All samples were replicated 3 times.

Quality by Design (QbD) Paradigm

● Construction of quality target product profile

A desired quality product could be ensured by achieving all the quality characteristics and properties that are required to be in a drug product. This could be achieved by ensuring the product's safety and efficacy; hence, the Quality Target Product Profile (QTPP) could be determined. The key element in achieving the QTPP is the appropriate determination

of the critical process parameters (CPP) and material attributes (CMA) [42].

As the main target in the current study was to enhance silymarin's bioavailability by enhancing its solubility, a thorough risk assessment study was conducted to determine the highest risk factors affecting the QTPP. It was found that a small vesicular size could increase the drug's solubility. Moreover, a better formulation performance could be reflected by its high drug encapsulation efficiency [42]. Hence, the highest risk factors affecting the QTPP in this study were the particle size and the entrapment efficiency. These were considered the critical quality attributes (CQA) in this work.

• Risk assessment

The target of any risk assessment study is to gather all data and the main risk factors that significantly enhance the QTPP. This study started with the identification of risk factors affecting the QTPP. This was followed by a risk analysis study in which the parameters were ordered according to their significance impact on the QTPP. Risk analysis was conducted through Ishikawa diagrams. Two Ishikawa diagrams were constructed, one for the particle size and the other for the EE% [43]. Further analysis of these diagrams showed that 6 critical process parameters and material attributes (CPP/CMA) affected the chosen CQA; thus, they were used for the screening design.

• Screening of CPP/CMA applying fractional factorial design

A 26–2 fractional factorial design was the design of choice in the screening step. Fractional factorial design is basically used to explore cause-and-effect relationships based on an economic point of view. It differentiates the main significant effects from the less important ones [44], so it is very beneficial in the screening step in QbD approach. The six CPP/CMA were XS1: time of cross-linking, XS2: albumin amount, XS3: pH of albumin solution, XS4: silymarin amount, XS5: volume of desolvating agent, and XS6: type of the solvent, which were all studied at 2 levels. This, in turn, led to the production of 16 formulae as shown in Table 1.

• Optimization of CPP/CMA applying D-optimal design

To find the optimum formulation, the most significant CPP/CMA that affected the CQA were deeply explored using a D-optimal design, while the rest of the CPP/CMA were kept constant at the levels that showed the best constraints. Accordingly, two CMA, namely X1: albumin amount and X2: silymarin amount, were deeply studied

through a D-optimal design. The D-optimal design was chosen as it minimizes the area of confidence, and can accommodate multiple types of factors [44]. Accordingly, 16 new formulations were suggested by the design to investigate the potential effects of these two CMA, together with their interactions, on the PS and the EE% as shown in Table 2.

Data Optimization and Model Validation

Desirability criteria were used by the software to select an optimized formula (O1), where the constraints were set to have the smallest particle size and the highest EE%. The optimized formula was prepared to be tested in terms of the previously mentioned CQA in order to calculate the % bias between the expected and observed results. Moreover, the optimized formula was tested in terms of polydispersity index (PDI), z-pot, TEM, in vitro release rate, stability study, and in vitro cytotoxicity.

Design Space and Control Strategy

In order to study the relationship between the variables (CMA on the CQA), a design space was created where the successful operating ranges were determined. Thus, operating within this range is expected to have a product with the desired properties [19].

The consistency and reproducibility of the product with the desired quality were further ensured through the control strategy [45].

Stability Study

The optimized formula was subjected to a stability study over a 3-month period. The PS, EE%, PDI, and z-pot were measured at 4 °C, as mentioned previously [39].

Assessment of the Effect of Silymarin as a Free Drug and in the Optimized Formula on the Proliferation of HepG2 Cells

The in vitro cytotoxicity of silymarin in the free form, and in the optimized formula, on the proliferation of HepG2 cells was measured using SRB assay. This method is based on the stoichiometric binding of SRB to the protein; thus, the amount of bound dye is the indicator for the cell mass and can be used as a measure of the cell proliferation. Aliquots of 100 µL cell suspension (5×10^3 cells) were seeded in 96-well plates and incubated in complete media for 24 h. Cells were treated with another aliquot of 100 µL media containing drug standard solution (dissolved in DMSO) or optimized formula (O1) at various concentrations: 0.1, 1, 10, 100, 1000 µM. After 72 h of drug exposure, cells were fixed by replacing media with 150 µL of 10% TCA and incubated

Table 1 Fractional factorial design, with levels and results from the screening step

	Lower level (-1)	Higher level (+1)
XS₁: Time of cross-linking (h)	2	24
XS₂: Albumin amount (mg)	50	200
XS₃: pH of albumin solution	8	9
XS₄: Silymarin amount (mg)	5	50
XS₅: Desolvating agent volume (mL)	8	12
XS₆: Type of solvent	Water	Solution of NaCl in water

Formula	XS_1	XS_2	XS_3	XS_4	XS_5	XS_6	PS (nm)	EE (%)
S_1	24	50	8	5	8	NaCl	159.0 ± 6.7	86.11 ± 4.2
S_2	24	200	9	50	12	NaCl	204.5 ± 5.6	82.20 ± 2.7
S_3	2	200	9	5	8	NaCl	95.5 ± 3.6	79.32 ± 4.6
S_4	2	50	8	50	12	NaCl	165.1 ± 4.9	88.73 ± 9.4
S_5	2	50	9	50	8	Water	187.0 ± 3.9	87.26 ± 4.7
S_6	2	200	8	5	12	Water	223.8 ± 9.8	89.29 ± 3.7
S_7	24	200	8	50	8	Water	150.1 ± 6.5	97.09 ± 4.7
S_8	24	50	9	5	12	NaCl	160.8 ± 7.4	26.19 ± 1.6
S_9	24	200	9	50	12	NaCl	208.8 ± 3.9	81.99 ± 4.8
S_{10}	24	50	8	5	8	NaCl	164.0 ± 6.7	86.26 ± 7.3
S_{11}	24	200	8	50	8	Water	154.9 ± 4.3	97.15 ± 3.6
S_{12}	24	50	9	5	12	Water	165.9 ± 3.9	25.49 ± 5.1
S_{13}	2	50	9	50	8	Water	190.5 ± 5.7	86.93 ± 4.9
S_{14}	2	200	8	5	12	Water	229.8 ± 4.6	80.70 ± 4.6
S_{15}	2	200	9	5	8	NaCl	99.9 ± 4.2	78.42 ± 7.3
S_{16}	2	50	8	50	12	NaCl	170.4 ± 3.5	88.68 ± 4.6

Results are expressed as mean ± S.D.

Table 2 D-Optimal design study with results from the optimization step

		Low level (-1)		High level (+ 1)	
X₁: Albumin amount (mg)		100		200	
X₂: Silymarin amount (mg)		5		50	

Formula	X_1	X_2	$Y_1 = PS$ (nm)	$Y_2 = EE$ (%)
F_1	200.0	5.0	176.6 ± 14.6	88.4 ± 3.8
F_2	127.0	50.0	186.6 ± 21.6	74.5 ± 9.4
F_3	127.0	50.0	186.0 ± 5.8	73.3 ± 4.6
F_4	181.5	12.8	151.0 ± 13.8	78.5 ± 1.8
F_5	197.5	30.7	188.9 ± 12.1	94.5 ± 3.4
F_6	200.0	50.0	152.4 ± 23.6	83.1 ± 9.5
F_7	100.0	5.0	180.7 ± 3.6	34.8 ± 4.7
F_8	200.0	5.0	175.8 ± 16.7	89.8 ± 3.7
F_9	120.18	16.09	121.7 ± 16.93	58.59 ± 5.76
F_{10}	163.50	41.33	179. ± 15.98	79.15 ± 7.18
F_{11}	100.00	33.17	189.2 ± 10.82	81.22 ± 6.27
F_{12}	147.00	5.00	223.1 ± 6.87	65.23 ± 7.34
F_{13}	100.00	5.00	180.6 ± 11.43	33.36 ± 5.87
F_{14}	156.00	21.53	140.0 ± 14.76	71.41 ± 6.98
F_{15}	200.00	50.00	152.3 ± 6.87	81.89 ± 6.99
F_{16}	100.00	33.17	189.1 ± 23.12	80.57 ± 3.88

Results are expressed as mean ± S.D.

at 4 °C for 1 h. The TCA solution was removed, and the cells were washed 5 times with distilled water. Aliquots of 70 μL SRB solution (0.4%w/v) were added and incubated in a dark place at room temperature for 10 min. Plates were washed 3 times with 1% acetic acid and allowed to air-dry overnight. Then, 150 μL of TRIS (10 mM) was added to dissolve protein-bound SRB stain. The absorbance was measured at 540 nm using a BMGLABTECH®-FLUOstar Omega microplate reader (Ortenberg, Germany). The percentage of cell growth was plotted versus the logarithm of drug concentration to determine the IC50, the drug concentration that causes 50% reduction in the cell growth.

The effects of silymarin as a free drug and in the optimized formula (O1) on the cell cycle of HepG2 cells were analyzed by flow cytometry. HepG2 cells (cultured in 12-well plates for 24 h) were treated with 100 μL media containing either free silymarin, or the optimized formula equivalent to a concentration equal to IC50. After 72 h of drug exposure, cells were detached from plates using the enzyme-free cell dissociation buffer, and fixed with 70% ethanol. The nucleic acid contents were stained with propidium iodide in RNase-containing buffer and analyzed on FACSVerse. Cell cycle (G0, G1, G2M, and S) was analyzed using FlowJo software (Becton and Dickinson, USA).

Data Analysis

Design-Expert 10.0.1.0® software (Stat-Ease Inc., Minneapolis, USA) was used for the statistical analysis of the fractional factorial design and D-optimal design by regression equations and analysis of variance (ANOVA). 3-D response surface plots were considered from the important tools used in the analyses. A p-value < 0.05 was considered significant [46]. In vitro cytotoxicity was analyzed using GraphPad Prism software package, version 5 (GraphPad Software, Inc., USA). All data was presented as mean ± SD.

Results and Discussion

Preparation of Albumin Nanoparticles

The desolvation technique was used for the preparation of albumin nanoparticles as this method is well known to create a less aggregated system, with a homogenous and stable distribution [47]. Ethanol was used as the desolvating agent, owing to its suitable dielectric constant and dipole moment, in addition to its excellent solubilizing property. In addition, ethanol passes through the hydrophobic region of the bovine serum albumin and disrupts the hydrophilic

layer of the protein in water, leading to the denaturation of the albumin, and hence the formation of the nanoparticles. Furthermore, as compared to other desolvating agents, ethanol is considered less toxic [39].

Glutaraldehyde was used as the cross-linking agent owing to its high reactivity and low cost, in addition to being a water-soluble bifunctional reagent. Glutaraldehyde is known to react with several functional groups of proteins, such as amine, thiol, phenol, and imidazole, because the most reactive amino acid side chains are nucleophiles [48]. The nucleophiles attack the ε-amino groups of lysine and arginine residues of the protein, where the cross-linking process takes place. Thus, the two carbonyl groups of glutaraldehyde make this and form Schiff bases which are unstable in acidic conditions and are very stable under basic conditions. Furthermore, glutaraldehyde is capable of forming both inter- and intracovalent bonds between the protein units or within them [9, 49].

It has been previously reported that in the preparation of albumin nanoparticles, the drug could be loaded during the preparation or after the formation of nanoparticles, by incubating the drug solution with the formed nanoparticles. The addition of the drug during the preparation will allow the drug to be embedded into the nanoparticles' matrix as well as to be adsorbed on the surface of the particles [2]. Encapsulating the drug into the nanoparticles could sustain the release of the drug, which satisfies the target of the current study to control the drug release in the blood circulation before reaching the site of action [50].

Quality Target Product Profile

Defining the QTPP is the first step in the QbD, which describes all the characteristics related to the quality that should be present in the product in order to achieve the main target of the study [51]. The entire steps of QbD followed in this study are illustrated in Fig. 2a, which enlists the whole phases taking place to achieve the target. QbD starts by defining the target of the study, which is the optimization of silymarin-albumin nanoparticles, to be used as an anticancer agent. This was followed by risk factor identification, and determination of the CQA, which were found to be PS and EE% in the current study. An experimental design was first developed by screening the main CPP/CMA that may have a direct significant impact on the CQA, using a fractional factorial design. Next was applying a D-optimal design to reach the optimal silymarin-loaded albumin nanoparticles. Then was the creation of a design space and control strategy, ending with continual improvement, with assurance of consistent quality, which was achieved by the further steps applied on the optimized silymarin-loaded albumin nanoparticles.
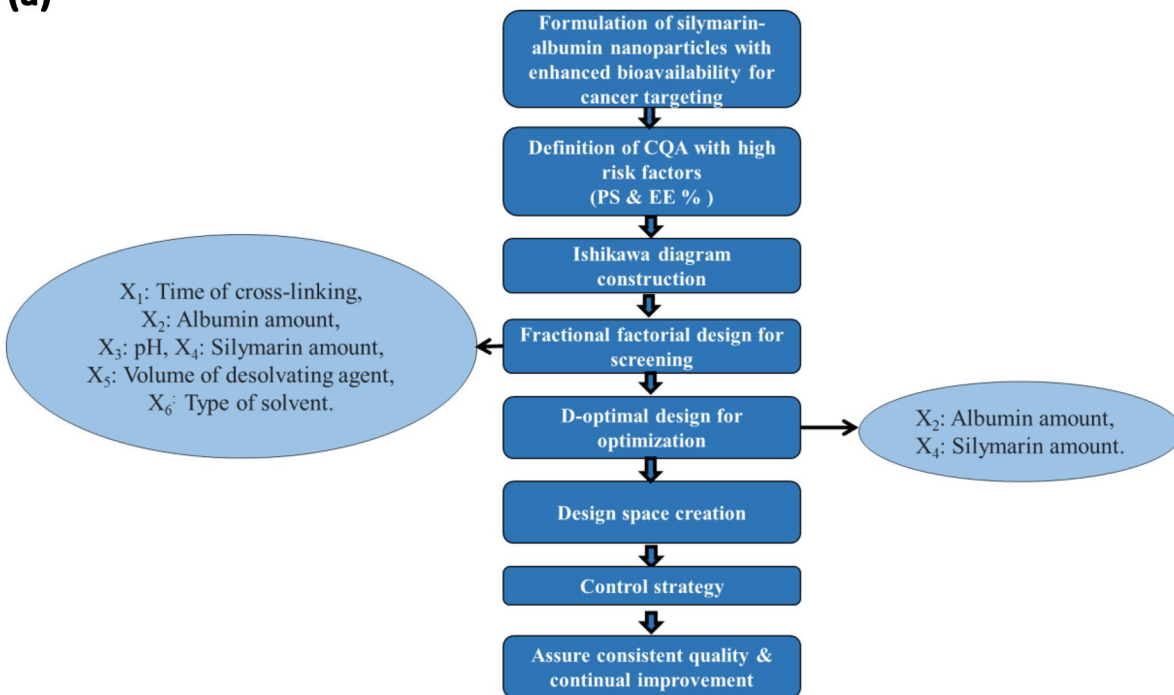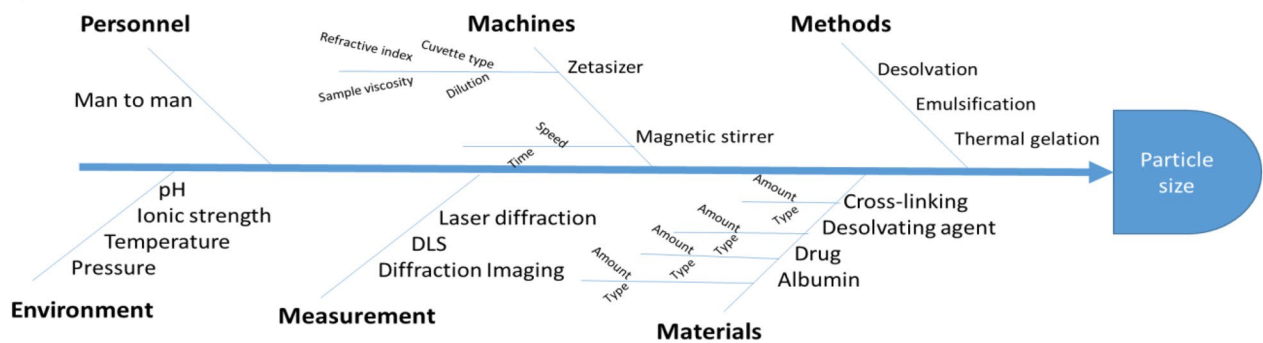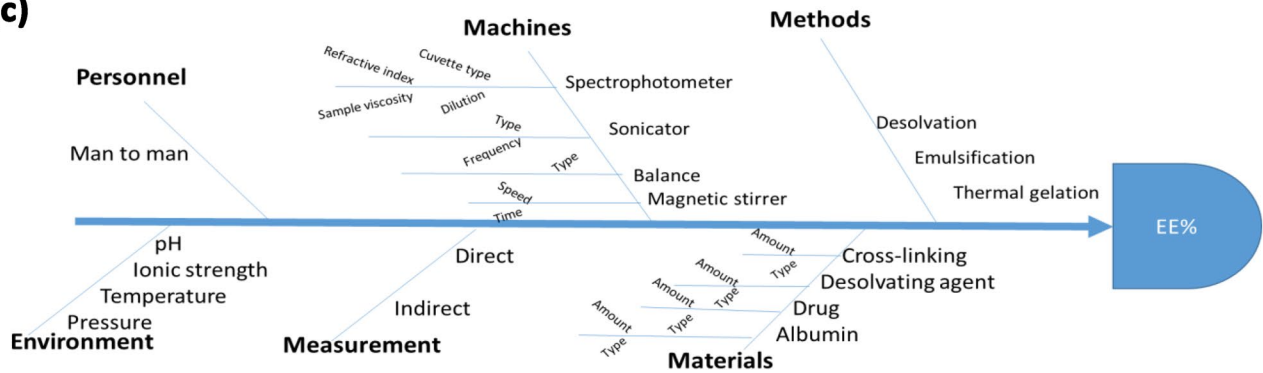
Fig. 2. **a** QTPP of silymarin-albumin nanoparticles, **b** Ishikawa diagram for the particle size, **c** Ishikawa diagram for the entrapment efficiency

Risk Assessment

Defining the QTPP could be assessed by determining the most critical parameters that when achieved may result in the desired drug product. Accordingly, in this study, these formulation parameters were the particle size and the drug entrapment efficiency. Consequently, a goal of the current study is to formulate albumin nanoparticles with the smallest vesicular size together with the highest EE%. A reduction in the vesicular size is expected to enhance the drug's solubility [52]; furthermore, the vesicular size has a dynamic role for targeting tumor tissues, where a size less than 400 nm can potentially target cancerous cells by the enhanced permeability and retention effect [2]. Moreover, a higher entrapment of the drug within the nanoparticles could reduce the manufacturing cost with a greater flexibility in dosing [53].

In order to facilitate risk assessment, Ishikawa diagrams were constructed to help in the identification of the potential risks and the corresponding causes [54]. Accordingly, two Ishikawa diagrams (cause and effect diagrams) were built (Fig. 2b, c) which show the whole factors that may contribute to the quality attribute, including methods, material, and machines used in the preparation and measurements, together with the personnel and environmental factors. One Ishikawa diagram was constructed for the particle size, and the other was constructed for the entrapment efficiency. Analyzing these diagrams resulted in the identification of six key variables, namely, time of cross-linking, albumin amount, pH of albumin solution, silymarin amount, desolvating agent volume, and the type of the solvent, which were recognized as high risk factors and were used for the screening study. The rest of the variables were kept at a constant level, and could be routinely controlled.

Screening Using Fractional Factorial Design

The levels of the six CPP/CMA were chosen based on preliminary experiments and based on previous literature. Several research studied the effect of the time of cross-linking and obtained different results [8, 39, 55], so thus would be studied deeply in the current study. Furthermore, the

albumin and the drug amount might have a direct impact on the studied CQA [50, 56–58]. The pH was chosen to be between 8 and 9, which is above the isoelectric point of albumin (4.7); as it is well reported that the particle size decreases with increasing the pH [39], so it would be screened if this difference would significantly affect the formulation of albumin nanoparticles. It was reported that the albumin nanoparticle formation process depends greatly on the volume of the desolvating agent added, which also may have a direct impact on the vesicular size [2, 8, 9, 37, 50, 55, 59, 60]. Moreover, the sodium chloride solution would be compared with water as the solvent to obtain the solvent that would not interfere with the desolvation and the cross-linking processes [39]. The CPP/CMA that most significantly affected the CQA were further analyzed to be more deeply deliberated in the optimization step.

To screen the most significant CPP/CMA affecting the albumin nanoparticles, a 26–2 fractional factorial design was conducted with six CPP/CMA each at two levels, resulting in 16 formulations (S1–S16). These formulations were prepared and characterized in terms of PS and the EE%, as tabulated in Table 1. Further analysis using ANOVA revealed that the particle size and the EE% were affected by all the CPP/CMA as represented in Table 3. The correlation coefficient $R2$ was found to be 0.999 for the PS and 0.904 for the EE%, giving a significant fitting to the model.

As can be observed from Table 3, the time of cross-linking (XS1) had a negative impact on the EE%, where a short time of cross-linking resulted in a higher EE%. As for the effect of albumin amount (XS2), it was observed that increasing the albumin amount resulted in a significant increase in both the particle size and the EE%. The relationship between the albumin amount was not linear with the PS or the EE%, and thus would be deeply studied in the further optimization step. Similar results were obtained by [61].

The pH of the albumin solution (XS3) significantly affected both the PS and the EE%. A smaller vesicular size was observed as the pH increased from 8 to 9: this could be attributed to the extension of the BSA backbone with loose unordered parts, by increasing the pH, allowing charged side chains to be accessible [62], which in turn increases

Table 3 ANOVA study of the fractional factorial design

	Y_1: PS (nm)		Y_2: EE (%)	
	Coefficient	*p*-value	Coefficient	*p*-value
β_0	+170.69	<0.0001	+78.87	0.0010
XS$_1$: Time of cross-linking (hr)	+0.31	0.05310	−6.05	0.0278
XS$_2$: Albumin amount (mg)	+0.35	0.03100	+6.91	0.0156
XS$_3$: pH	−6.45	<0.0001	−10.39	0.0017
XS$_4$: Silymarin amount (mg)	+8.22	<0.0001	+9.89	0.0023
XS$_5$: Desolvating agent volume (mL)	+20.45	<0.0001	−8.46	0.0056
XS$_6$: Type of solvent	−12.16	<0.0001	+5.10	0.0537

the surface charge and reduces the particle attraction and agglomeration, leading to a reduction in the vesicular size [63]. This finding was in accordance with [37]. However, the higher pH resulted in a lower EE%, which could be due to more ionization of the protein at the higher pH, resulting in the hindrance of the incorporation of the drug into the nanoparticles due to the surface charge at that pH, and hence a lower EE% [55]. Furthermore, at high pH, less particle yield could be obtained, which could reduce the incorporation of the drug due to insufficient particle formation [37].

A larger particle size with higher EE% was observed as the drug amount (XS4) increases; however, the relationship was not linear, and thus would be deeply studied in the optimization step. These results were in accordance with that obtained by [61].

The increase in the volume of the desolvating agent (XS5) resulted in a significant increase in the vesicular size, which could be attributed to the direct relationship between the volume of non-solvent and the hydration of the protein. Large amounts of the desolvating agent might reduce the hydration of the albumin, with the consequence of the reduction in the dielectric constant (DEC) of the whole solution [8], which finally increases the vesicular size. It was previously reported that when the volume of the non-solvent is small, it will be insufficient to make the solute reach its supersaturation point; thus, precipitation will not occur efficiently, leading to deformation of the particles [55], and hence an increase in the vesicular size. Furthermore, as stated by Yoshikawa et al. (2012), the increase in the percentage of desolvating agent above 80% may lead to a dramatic change in the structure of protein, which in turn may increase the vesicular size [64]. Moreover, a less entrapment of the drug was observed as the volume of the desolvating agent increased. This could be attributed to the insufficient hydration of the protein, which might not give it the chance to form sufficient nanoparticles, resulting in small yield of the nanoparticles [55].

Sodium chloride solution had a less significant impact than water on increasing the particle size (XS6), which could be due to the higher ionic strength of sodium chloride solution over that of water. This, in turn, reduces the surface

charge on the albumin nanoparticles, with the consequence of reducing the electrostatic repulsion between the particles due to the charge screening by the addition of the ions, and the subsequent reduction in the electrophoretic mobility [55]. Accordingly, sodium chloride solution would be used to prepare the albumin nanoparticles in the subsequent optimization step.

As mentioned previously, the constraints of the current study were to attain a small particle size and a high EE%. Thus, the CPP/CMA were all set at constant levels which achieve the aforementioned constraints, except the albumin amount and the drug amount that will be studied deeply in the optimization step. Accordingly, the pH was chosen to be set at 8, as its effect on the PS was greater than on the EE%, with the least time of cross-linking, and the least volume of the desolvating agent.

D-optimal Design Analysis

The results of the PS and the EE%, from the D-optimal design, were fitted to polynomial cubic models. The linear regression equations showing the effect of each of the studied CMA, and their interactions on the PS and EE%, are represented in Table 4. A perfect fit of the model was obtained as indicated by the correlation coefficient (R2) values. Perfect results were obtained between the adjusted R2 and the predicted R2, together with an adequate precision greater than 4, indicating an adequate signal, and assuring the ability of the model to navigate the design space.

Further analysis using ANOVA showed significant models of each of the PS, and the EE% at p-level < 0.05, with a non-significant lack of fit as represented in Table 5.

Particle Size Analysis

It has been reported that nanoparticles smaller than 200 nm decrease phagocytic uptake due to opsonization. This, in turn, enhances drug targeting to cancerous cells. Accordingly, one of the main goals of the current study is to obtain a particle size less than 200 nm [65]. Furthermore, a study

Table 4 Regression equations, R^2, adjusted R^2, predicted R^2, and adequate precision as obtained from D-optimal design

	PS	EE%
Regression equation	P.S. = +20.41*A + 64.44*B − 21.59*AB + 5.43*A^{2}78.59*B^2 +61.39*A^2 − 56.40*AB^2 − 2.54*A^3 − 142.61*B^3 (4)	EE% = +74.0 + 8.83*A + 18.35*B − 17.04*AB + 6.05 (5) *A^2 − 5.40*B^2 + 13.36*A^{2}B + 4.73*A^3 − 20.41*B^3
R^2	0.9999	0.9986
Adjusted R^2	0.9998	0.9971
Predicted R^2	0.9533	0.9910
Adequate precision	372.467	84.232

Table 5 ANOVA study of the D-optimal design

Source	PS					EE%				
	Sum of squares	df	Mean square	F value	p-value Prob > F*	Sum of squares	df	Mean square	F value	p-value Prob > F*
Model	8891.41	9	987.93	8296.40	<0.0001	4656.51	8	582.06	636.76	<0.0001
X_1-Albumin Conc	141.44	1	141.44	1187.80	<0.0001	29.77	1	29.77	32.56	0.0007
X_2-Drug amount	1527.95	1	1527.95	12,831.34	<0.0001	129.09	1	129.09	141.23	<0.0001
X_1X_2	1410.43	1	1410.43	11,844.42	<0.0001	958.07	1	958.07	1048.10	<0.0001
X_1^2	45.98	1	45.98	386.15	<0.0001	77.65	1	77.65	84.94	<0.0001
X_2^2	5280.05	1	5280.05	44,340.43	<0.0001	25.80	1	25.80	28.22	0.0011
$X_1^2X_2$	2254.73	1	2254.73	18,934.63	<0.0001	166.11	1	166.11	181.71	<0.0001
$X_1X_2^2$	1904.04	1	1904.04	15,989.62	<0.0001					
X_1^3	1.90	1	1.90	15.95	0.0072	6.56	1	6.56	7.17	0.0316
X_2^3	4231.34	1	4231.34	35,533.64	<0.0001	86.79	1	86.79	94.94	<0.0001
Residual	0.71	6	0.12			6.40	7	0.91		
Lack of Fit	0.37	1	0.37	5.51	0.0658	2.74	2	1.37	1.88	0.2468
Pure Error	0.34	5	0.068			3.66	5	0.73		
Cor Total	8892.12	15				4662.91	15			

*Significance was considered at p-value < 0.05

showed that the pore size of the capillaries supplying the tumor cells is about 400 nm; thus, nanoparticles with vesicular size less than 400 nm could increase the residence time of the nanoparticles in the systemic circulation, and would passively target the tumor cells through the enhanced permeability and retention effect [2].

As observed from Table 2, particle size ranged from 121.7 ± 16.9 to 223.1 ± 6.8 nm. Further ANOVA analysis showed that the individual effect of each of the studied CMA and their interactions significantly affected the particle size as represented in Table 5. A larger particle size was obtained as the albumin amount (X1) or the drug amount increased (X2), as observed from the positive coefficients in Eq. 4 in Table 4.

The larger size of the albumin nanoparticles due to the increase in the albumin amount (X1) might be attributed to the formation of a stronger intermolecular disulfide bond at the higher albumin concentration. This, in turn, resulted in a greater aggregation of the protein, and hence a larger-sized albumin nanoparticle [50]. Moreover, better hydrophobic interaction takes place at an increased albumin amount, which leads to an increase in the protein coagulation, and finally an increase in the size of the albumin nanoparticles [57]. Furthermore, at a higher BSA concentration, the viscosity increases, which slows down the frequency of transport of the protein from water to ethanol, resulting in a slower nucleation rate and a bigger vesicular size [55].

The positive impact of the silymarin amount (X2) on the particle size could be attributed to the poor solubility of silymarin in water (< 50 μg/mL) [66]. This poor solubility will allow the drug to be incorporated into the protein's matrix during the desolvation process. As a result, a kind of hydrophobic interaction between the drug and the protein will occur, which increases the vesicular size of the nanoparticles [57]. Moreover, at a high drug amount, no protein binding sites would be available, and thus silymarin would be forced to interact with the nanoparticles at the protein's surface, causing an increase in the vesicular size [58]. As can be deduced from Eq. 4 in Table 4, there was an antagonistic effect between the albumin amount and the drug amount.

As can be observed from Fig. 3a, a cubic model existed between each of the CQA and the studied CMA. The 3-D plot showed an initial reduction in the particle size as each of the albumin amount or the drug amount increased. This was followed by an increase in the particle size with a further increase in both CMA.

Entrapment Efficiency Analysis

The percentage yield for all formulations were found to be from 93.67 ± 3.7 to 98.77 ± 1.87. whereas, the drug loading % was found to be from $40.31\% \pm 2.76$ to $77.65 \pm 5.65\%$.

A major goal of the current study is to maximize the entrapment of the drug into the nanoparticles in order to increase the drug concentration at the site of action [50].

As observed in Table 2, the EE% ranged from $33.36\% \pm 5.8$ to $94.57\% \pm 3.4$, with a cubic best fitting model as represented in Table 5. The entrapment efficiency was found to increase by increasing each of the albumin amount (X1) and the drug amount (X2) individually, as observed in Eq. 5 in Table 4. The increase in the EE% at a higher albumin amount is due to the higher availability of the albumin surrounding the drug [67]. As the albumin concentration increases, more nanoparticles would be formed, which in turn increases the chance for better drug encapsulation.

A higher EE% was observed when the drug amount increased. This may be due to the higher interaction of the drug with the active sites in the protein at the higher drug amount, causing a higher EE% [58]. Moreover, a larger particle size was observed with the increase in the drug amount, which gives a larger volume of the nanoparticles to encapsulate more drug [56].

Equation 5 shows a negative coefficient of XAB, indicating a synergistic effect between the studied MA on the EE%. Figure 3b shows the non-linear effect of each of the albumin amount and the drug amount.

Data Optimization and Model Validation, Design Space, and Control Strategy

A design space was constructed based on the key parameters discussed earlier, as represented in Fig. 3c. It shows two regions: a yellow region where working within this region is expected to get the desirable outcomes, and a gray region which shows the undesirable limits. A desirability approach based on a numerical technique was employed to get an optimized formula [18]. Accordingly, a new formula (O1) was chosen, with a desirability of 0.859.

A control space has been established, showing the highest and lowest limits for the MA and CQA, which also ensures the reproducibility of CMA and CQA that could be routinely controlled. Table 6 shows the optimized formula (O1), together with the expected results as suggested by the software. The optimized formula was prepared and characterized in terms of particle size and EE% to calculate the % bias [68]. The low % bias indicates the validity of the design.

$$* \%\text{bias} = \frac{(|Expected - Observed|)}{Expected} * 100$$

Fig. 3. **a** 3-D response surface plot of the particle size, **b** 3-D response surface plot of the entrapment efficiency, **c** design space of silymarin-albumin nanoparticles
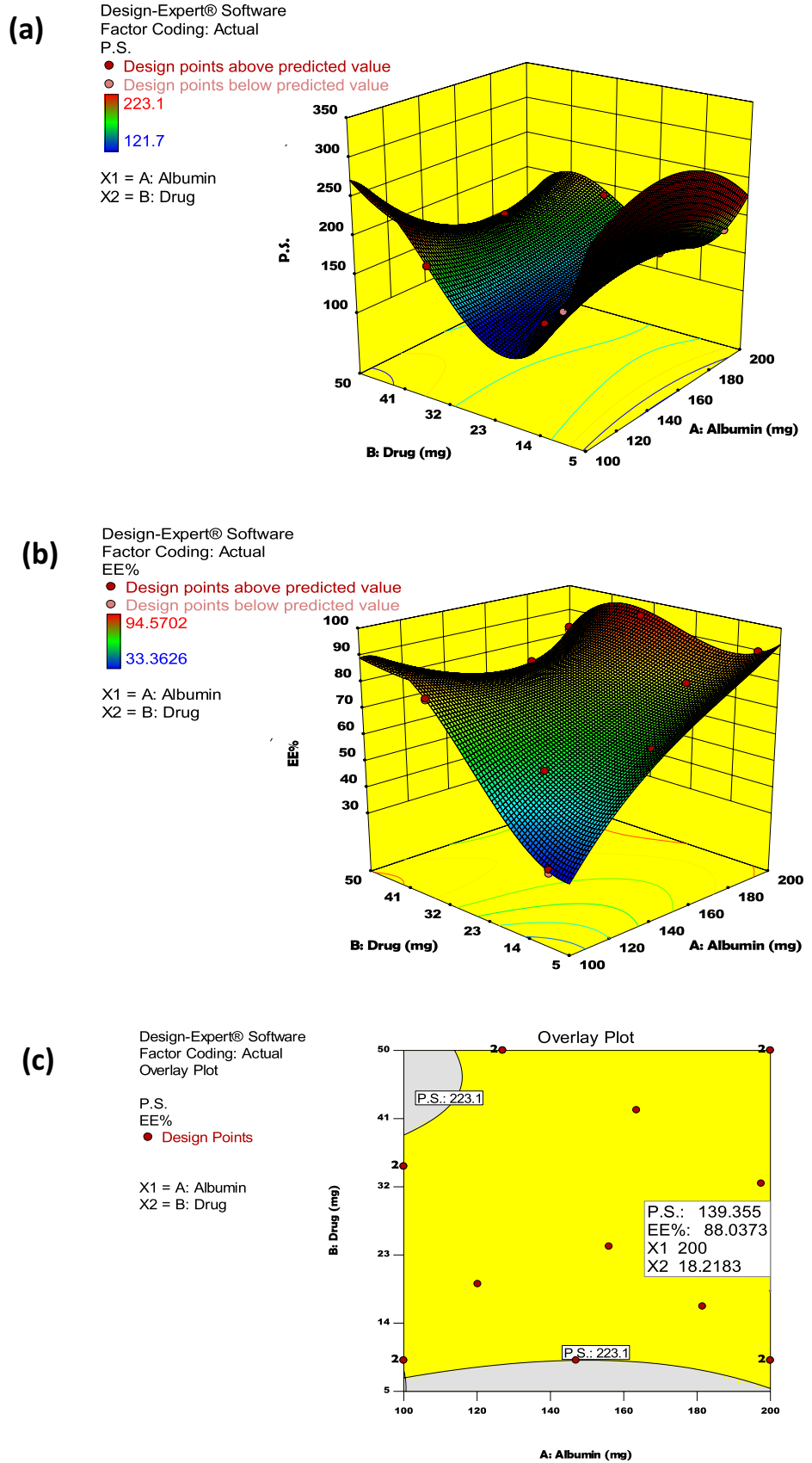
Table 6 The optimized formula with the expected and the observed results

	Albumin amount (mg)	Drug amount (mg)	PS (nm)	EE (%)
	200	18.2		
Expected results			139.350	88.084
Observed results			135.3 ± 7.9	88.1 ± 2.9
% bias*			2.901%	0.086%

Characterization Tests on the Optimized Formula

Transmission Electron Microscope Analysis

The morphological analysis of albumin nanoparticles in Fig. 4 shows spherical particles of about 100 nm ± 2.8, with a uniform particle size distribution, which coincides with the diffractive light scattering measurements (DLS). It should be mentioned that the slight difference between the diffractive light scattering (DLS) and the TEM might be attributed to the difference in the sample preparation. The DLS measures the hydrodynamic particle diameter, whereas the TEM measures the diameter of the particles in their dried states [39].

Zeta Potential and Polydispersity Index

Zeta potential gives an indication of the stability of the nanoparticles in the dispersion through electrostatic repulsion between the particles. As the value increases, it gives an indication of more repulsion between the nanoparticles, reducing the tendency of aggregation that could occur between the nanoparticles [2]. The zeta potential for the silymarin nanoparticles was found to be − 12.5 ± 1.2 mV. The negative charge might be due to the preparation of the albumin at a pH higher than the isoelectric point of the protein [69], leading to the ionization of the carboxyl terminal of the protein, and hence imparting a negative charge [39].

Polydispersity index was found to be 0.09 ± 0.007, which indicates the homogeneity of the size distribution within the formed nanoparticles.

In Vitro Drug Release

The release of silymarin from both the standard solution and the optimized formula (O1) is shown in Fig. 5. The release of silymarin from albumin nanoparticles showed a biphasic release, with an initial burst effect, which is followed by a sustained release over 48 h. A sudden burst release of about 45% was observed within 4 h from O1, followed by a slower release over the 48 h, whereas the standard drug was completely released within 3 h. The initial burst effect might be due to the free unencapsulated drug and the drug on the surface of the nanoparticles. The sustained release pattern may be attributed to the drug incorporated in the core of the nanoparticles' matrix. It should be mentioned that the sustained release effect is in great favor for the cancer targeting as it is required for the anticancer drugs to have a slow release in the blood to reduce its side effects on the normal cells, whereas when it reaches the cancer cells, it should be high [2].
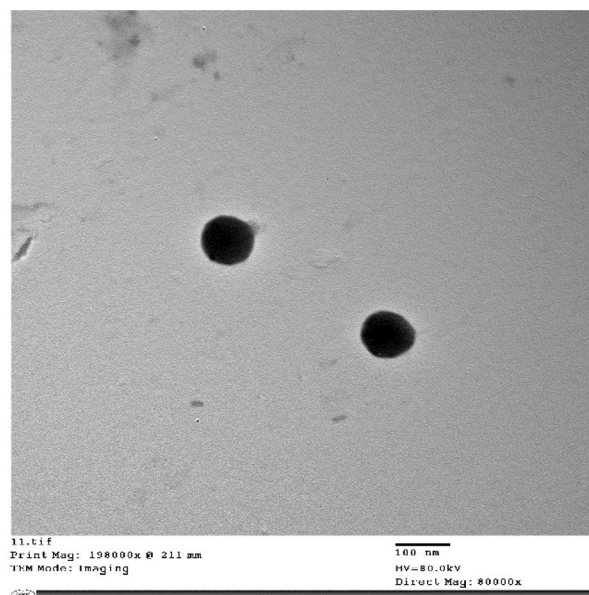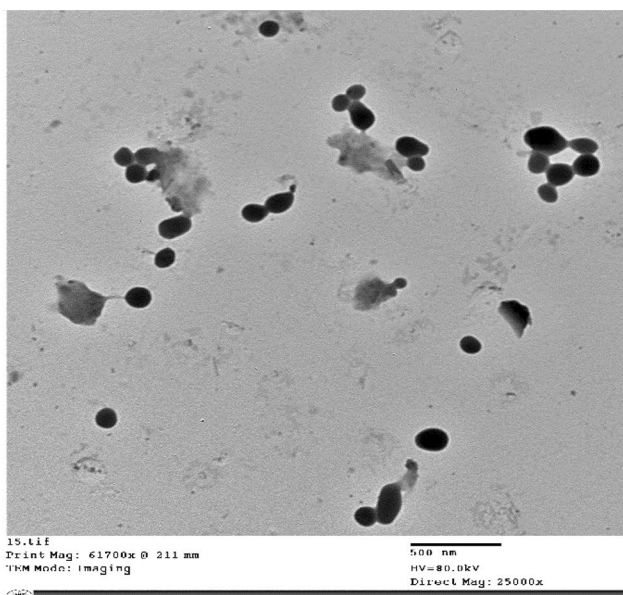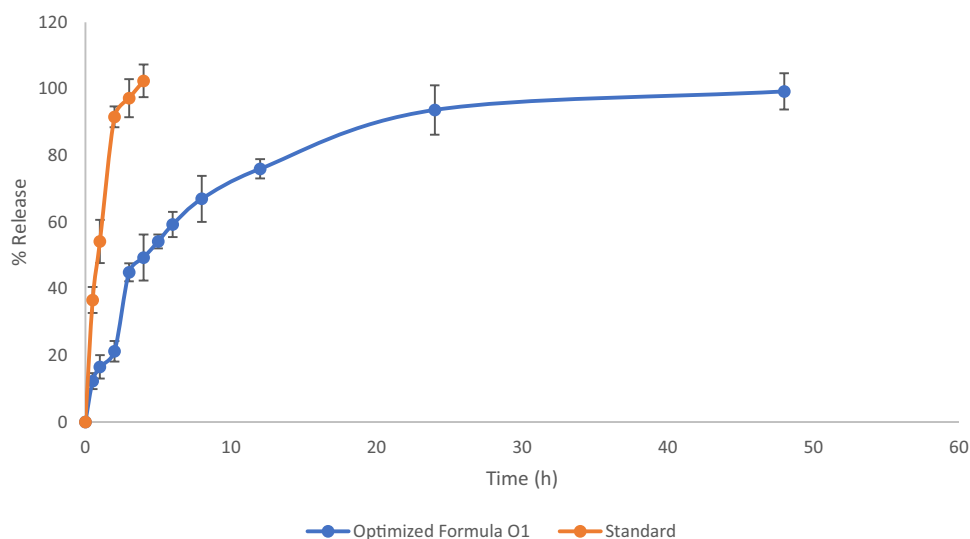

Fig. 4 TEM micrographs of the optimized silymarin-albumin nanoparticles

Fig. 5 Release pattern of silymarin from the optimized formula and standard silymarin

Stability Testing

The values of the PS, EE%, PDI, and z-pot of the optimized formula after a 3-month storage at 4 °C were 133.01 ± 2.7 nm, $85.64 \pm 0.4\%$, 0.09 ± 0.1, and -11.94 ± 0.9 mV respectively. The results of the stored samples show no significant difference as compared to the freshly prepared ones. This validates the stability of the formulation at 4 °C.

Molecular Docking

In an attempt to explore the molecular basis behind the observed cytotoxic activity, silymarin was docked in the active site of bovine serum albumin obtained from the protein databank (PDB ID: 4JK4) using MOE software version 2014.0910.

The docking scores in (kcal/mol) and major interactions of silymarin are provided in Table 7 and Fig. 1b along with the score and interactions of the native compound of the albumin.

Table 7 Docking scores and major interactions. The amino acid with which the ligand interacts with is provided below the relevant interactions

| Ligand	Score (kcal/mol)	Interactions
Native ligand	-5.39686871	Arg 217
		Arg 256
		Tyr 149
Silymarin	-5.44053364	Arg 217
		Arg 256
		Tyr 149
		Asp 450

As depicted in both Table 7 and Fig. 1b, it is clear that silymarin displays similar interactions as the native ligand with the essential amino acids Arg 217, Arg 256, and Tyr 149. Additional interaction with Asp 250 was found with silymarin.

Antiproliferative Effects of Silymarin on HepG2 Cells

Silymarin has been used for centuries as a hepatoprotective agent and its anticancer effects on various malignancies have been reported. Silymarin was shown to suppress the proliferation of a variety of tumor cells, including prostate, ovarian, breast, lung, skin, liver, and bladder [70–75].

The effects of free silymarin and albumin-based silymarin on the proliferation of HepG2 cells for 72 h were examined by SRB assay. According to Fig. 6 and Table 8, both free silymarin and the optimized formula significantly ($p < 0.05$) inhibited the growth of HepG2 cells in a concentration-dependent manner. The IC50 for the optimized formula was lower than that of the free drug (84 μM versus 140 μM, respectively). This indicates that the optimized formula was more effective in the inhibition of the proliferation and in the induction of apoptosis in the human hepatocellular carcinoma cell line HepG2 than the free drug. A lower IC50 of the optimized formula and a pronounced cell death were observed in the flow cytometric analysis, as compared to the free drug. Twenty percent of the cells with reduced DNA content (Sub-Go peak) were markedly observed which indicates apoptosis. The effects of free silymarin and the optimized formula on the cell cycle of HepG2 cells were assessed after exposing the cells to 140 μM of both for 72 h. A significant suppression of the S phase was observed after treating the HepG2 cell with the optimized formula.

Fig. 6 Effects of silymarin as free drug (standard silymarin) and in the optimized formula on the proliferation of HepG2 cells. Cells were treated for 72 h with 1000 µM of free silymarin or the optimized formula; control cells were treated with DMSO. The cell growth was assessed by SRB assay
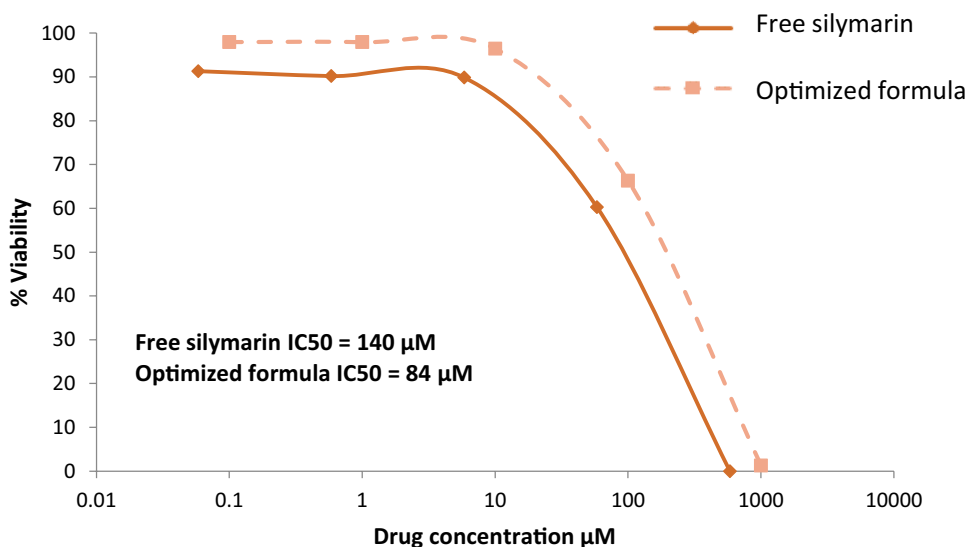
However, no suppression of the S phase was observed after treating the HepG2 cell with the free drug. In addition, a pronounced proportion of dead cells (20.7 ± 0.6) was also observed after treating the HepG2 cell with the optimized formula. This could be attributed to that silymarin could induce G0/G1-phase arrest with a concomitant decrease in the percentage of cells in the S-phase of the cell cycle [72]. Moreover, silymarin could induce inhibition and apoptotic cell death in carcinoma cells [76]. Furthermore, silymarin could inhibit the proliferation of human prostate carcinoma PC3 cells, induce cell death, and cause G1 cell cycle arrest and suppression of S phase [74]. In addition to that, silymarin may have an effect on the growth of the hepatocellular carcinoma cells, in addition to the increase of apoptotic cell percentage, and the proportion of cells with reduced DNA content (Sub-Go peak), with loss of cells in the G1 phase [75].

Table 8 Effect of silymarin as a free drug and in the optimized formula on cell cycle distribution in human hepatocellular carcinoma cells (HepG2)

	G1 phase	S phase	G2/M phase	SubGo
Control	50.5 ± 2.0	26.9 ± 2.0	18.8 ± 0.4	1.7 ± 0.6
Free silymarin	59.1 ± 0.8	23.9 ± 0.7	11.8 ± 0.3	$3.2 \pm 0.1^*$
Optimized formula	41.0 ± 1.5	$18.0 \pm 0.8^*$	18.9 ± 1.2	$20.7 \pm 0.6^*$

Data are presented as mean $\pm$ S.D. of percent cell population in different phases of cell cycle

**p*-value < 0.05

Conclusion

The current study focused on the formulation and optimization of albumin nanoparticles, encapsulating a poorly water-soluble drug, silymarin, with the aim of enhancing its solubility and bioavailability, using a quality by design approach. A deep product and process understanding was accomplished using several tools as a complete risk assessment study that showed the most influential CPP/CMA affecting the CQA, which were found to be the albumin amount and the drug amount. Each of these CMA had a direct effect on the PS and the EE%. The study resulted in the creation of a design space and a control strategy. The optimized albumin-based formula showed promising results when further tested in terms of its morphology, in vitro release, and stability. The optimized albumin-based silymarin nanoparticles were tested for its effectiveness against hepatocellular carcinoma, and showed promising results when compared with the free silymarin, as indicated by the suppression of the S phase, after treating the HepG2 cell. Thus, successful silymarin-loaded albumin nanoparticles were prepared, and QbD was found to be a successful approach for its comprehensive and deep understanding.

Data Availability The datasets generated during and/or analysed during the current study are available from the corresponding author on reasonable request.

Declarations

Statement of Human and Animal Rights This article does not contain any studies with human or animal subjects performed by any of the authors. However the work was approved by MSA's ethical committee (#PT15/EC15/2019).

Conflict of Interest The authors declare no competing interests.

References

1. Patra JK, Das G, Fraceto LF, Campos EVR, Rodriguez-Torres MDP, Acosta-Torres LS, et al. Nano based drug delivery systems: recent developments and future prospects 10 technology 1007 nanotechnology 03 chemical sciences 0306 physical chemistry (incl. Structural) 03 chemical sciences 0303 macromolecular and materials chemistry 11 medical and He. J Nanobiotechnol [Internet]. BioMed Central. 2018;16:1–33. Available from: https://doi.org/10.1186/s12951-018-0392-8

2. Wilson B, Ambika TV, Dharmesh Kumar Patel R, Jenita JL, Priyadarshini SRB. Nanoparticles based on albumin: preparation, characterization and the use for 5-flurouracil delivery. Int J Biol Macromol [Internet]. Elsevier BV. 2012;51:874–8. Available from: https://doi.org/10.1016/j.ijbiomac.2012.07.014

3. Maitz MF. Applications of synthetic polymers in clinical medicine. Biosurface and Biotribology [Internet]. Elsevier. 2015;1:161–76. Available from: https://doi.org/10.1016/j.bsbt.2015.08.002

4. Karlsson J, Vaughan HJ, Jordan GJ. Biodegradable polymeric nanoparticles for therapeutic cancer treatments. Physiol Behav. 2015;176:100–6.

5. Takeuchi H, Yamamoto H, Kawashima Y. Mucoadhesive nanoparticulate systems for peptide drug delivery. Adv Drug Deliv Rev. 2001;47:39–54.

6. An FF, Zhang XH. Strategies for preparing albumin-based nanoparticles for multifunctional bioimaging and drug delivery. Theranostics. 2017;7:3667–89.

7. Khan I, Saeed K, Khan I. Nanoparticles: Properties, applications and toxicities. Arab J Chem [Internet]. The Authors. 2019;12:908–31. Available from: https://doi.org/10.1016/j.arabjc.2017.05.011

8. Von Storp B, Engel A, Boeker A, Ploeger M, Langer K. Albumin nanoparticles with predictable size by desolvation procedure. J Microencapsul. 2012;29:138–46.

9. Bronze-Uhle ES, Costa BC, Ximenes VF, Lisboa-Filho PN. Synthetic nanoparticles of bovine serum albumin with entrapped salicylic acid. Nanotechnol Sci Appl. 2017;10:11–21.

10. Hashem L, Swedrowska M, Vllasaliu D. Intestinal uptake and transport of albumin nanoparticles: potential for oral delivery. Nanomedicine. 2018;13:1255–65.

11. Ibrahim NK, Desai N, Legha S, Soon-Shiong P, Theriault RL, Rivera E, et al. Phase I and pharmacokinetic study of ABI-007, a Cremophor-free, protein-stabilized, nanoparticle formulation of paclitaxel. Clin Cancer Res. 2002;8:1038–44.

12. Karimi M, Bahrami S, Ravari SB, Zangabad PS, Mirshekari H, Bozorgomid M, et al. Albumin nanostructures as advanced drug delivery systems. Expert Opin Drug Deliv. 2016;1609–23.

13. Tian J, Liu J, Tian X, Hu Z, Chen X. Study of the interaction of kaempferol with bovine serum albumin. J Mol Struct. 2004;691:197–202.

14. Vega-Vásquez P, Mosier NS, Irudayaraj J. Nanoscale drug delivery systems: from medicine to agriculture. Front Bioeng Biotechnol. 2020;8:1–16.

15. Hossen S, Hossain MK, Basher MK, Mia MNH, Rahman MT, Uddin MJ. Smart nanocarrier-based drug delivery systems for cancer therapy and toxicity studies: a review [Internet]. J Adv Res Cairo University. 2019. Available from: https://doi.org/10.1016/j.jare.2018.06.005

16. Kamboj S, Chopra S. Quality by design (QBD) in pharmaceutical industry. Int J Curr Pharm Rev Res. 2015;6:142–8.

17. Yu LX, Amidon G, Khan MA, Hoag SW, Polli J, Raju GK, et al. Understanding pharmaceutical quality by design. AAPS J. 2014;16:771–83.

18. Patwardhan K, Asgarzadeh F, Dassinger T, Albers J, Repka MA. A quality by design approach to understand formulation and process variability in pharmaceutical melt extrusion processes. J Pharm Pharmacol [Internet]. 2015;67:673–84. Available from: https://doi.org/10.1111/jphp.12370

19. Xu X, Khan MA, Burgess DJ. A quality by design (QbD) case study on liposomes containing hydrophilic API: II. Screening of critical variables, and establishment of design space at laboratory scale. Int J Pharm [Internet]. Elsevier BV. 2012;423:543–53. Available from: https://doi.org/10.1016/j.ijpharm.2011.11.036

20. ICH Expert Working Group. Pharmaceutical Development Q8. ICH Harmon Tripart Guidel. 2009;1–28.

21. Rijcken CJF, Veldhuis TFJ, Ramzi A, Meeldijk JD, Van Nostrum C, Hennink WE. Novel fast degradable thermosensitive polymeric micelles based on PEG-block-poly(N-(2-hydroxyethyl)methacrylamide-oligolactates). Biomacromolecules. 2005;6:2343–51.

22. Senapati S, Mahanta AK, Kumar S, Maiti P. Controlled drug delivery vehicles for cancer treatment and their performance. Signal Transduct Target Ther. 2018;3:1–19.

23. Yetisgin AA, Cetinel S, Zuvin M, Kosar A, Kutlu O. Delivery applications. Molecules. 2020.

24. Demain AL, Vaishnav P. Natural products for cancer chemotherapy. Microb Biotechnol. 2011;4:687–99.

25. Wu JW, Lin LC, Tsai TH. Drug-drug interactions of silymarin on the perspective of pharmacokinetics. J Ethnopharmacol. 2009;121:185–93.

26. Javed S, Kohli K, Ali M. Reassessing bioavailability of silymarin. Altern Med Rev. 2011;16:239–49.

27. Sun N, Wei X, Wu B, Chen J, Lu Y, Wu W. Enhanced dissolution of silymarin/polyvinylpyrrolidone solid dispersion pellets prepared by a one-step fluid-bed coating technique. Powder Technol. 2008;182:72–80.

28. Song IS, Nam SJ, Jeon JH, Park SJ, Choi MK. Enhanced bioavailability and efficacy of silymarin solid dispersion in rats with acetaminophen-induced hepatotoxicity. Pharmaceutics. 2021;13.

29. Kumar, B. Solid dispersion- a review. PharmaTutor [Internet]. 2017;5:24–9. Available from: https://www.pharmatutor.org/articles/solid-dispersion-review

30. He J, Hou S, Lu W, Zhu L, Feng J. Preparation, pharmacokinetics and body distribution of silymarin-loaded solid lipid nanoparticles after oral administration. J Biomed Nanotechnol. 2007;3:195–202.

31. Cengiz M, Kutlu HM, Burukoglu DD, Ayhanci A. A comparative study on the therapeutic effects of silymarin and silymarin-loaded solid lipid nanoparticles on D-GaIN/TNF-α-induced liver damage in Balb/c mice. Food Chem Toxicol [Internet]. 2015;77:93–100. Available from: https://doi.org/10.1016/j.fct.2014.12.011

32. Ghasemiyeh P, Mohammadi-Samani S. Solid lipid nanoparticles and nanostructured lipid carriers as novel drug delivery systems: applications, advantages and disadvantages. Res Pharm Sci. 2018;13:288–303.

33. Yanyu X, Yunmei S, Zhipeng C, Qineng P. The preparation of silybin-phospholipid complex and the study on its pharmacokinetics in rats. Int J Pharm. 2006;307:77–82.

34. Tung NT, Tran CS, Nguyen HA, Nguyen TD, Chi SC, Pham DV, et al. Formulation and biopharmaceutical evaluation of supersaturatable self-nanoemulsifying drug delivery systems containing silymarin. Int J Pharm [Internet]. Elsevier. 2019;555:63–76. Available from: https://doi.org/10.1016/j.ijpharm.2018.11.036

35. Morakul B. Self-nanoemulsifying drug delivery systems (SNEDDS): an advancement technology for oral drug delivery. Pharm Sci Asia. 2020;47:205–20.

36. Fenyvesi F, Petervari M, Nagy L, Keki S, Zsuga M, Bacskay L, et al. Solubility increasing experiments of sylimarin with cyclodextrins. J Med Arad. 2011;14:13–7.

37. Langer K, Balthasar S, Vogel V, Dinauer N, Von Briesen H, Schubert D. Optimization of the preparation process for human serum albumin (HSA) nanoparticles. Int J Pharm. 2003;257:169–80.

38. Chhonker YS, Prasad YD, Chandasana H, Vishvkarma A, Mitra K, Shukla PK, et al. Amphotericin-B entrapped lecithin/chitosan nanoparticles for prolonged ocular application. Int J Biol Macromol. 2015;72:1451–8.

39. Piazzini V, Landucci E, D'Ambrosio M, Tiozzo Fasiolo L, Cinci L, Colombo G, et al. Chitosan coated human serum albumin nanoparticles: a promising strategy for nose-to-brain drug delivery. Int J Biol Macromol [Internet]. Elsevier BV. 2019;129:267–80. Available from: https://doi.org/10.1016/j.ijbiomac.2019.02.005

40. Lazaridou M, Christodoulou E, Nerantzaki M, Kostoglou M, Lambropoulou DA, Katsarou A, et al. Formulation and in-vitro characterization of chitosan-nanoparticles loaded with the iron chelator deferoxamine mesylate (DFO). Pharmaceutics. 2020;12.

41. Sebak S, Mirzaei M, Malhotra M, Kulamarva A, Prakash S. Human serum albumin nanoparticles as an efficient noscapine drug delivery system for potential use in breast cancer: preparation and in vitro analysis. Int J Nanomedicine. 2010;5:525–32.

42. Shah B, Khunt D, Bhatt H, Misra M, Padh H. Application of quality by design approach for intranasal delivery of rivastigmine loaded solid lipid nanoparticles: effect on formulation and characterization parameters. Eur J Pharm Sci [Internet]. Elsevier BV. 2015;78:54–66. Available from: http://linkinghub.elsevier.com/retrieve/pii/S0928098715003231

43. Xu X, Costa AP, Khan MA, Burgess DJ. Application of quality by design to formulation and processing of protein liposomes. Int J Pharm [Internet]. Elsevier BV. 2012;434:349–59. Available from: https://doi.org/10.1016/j.ijpharm.2012.06.002

44. Pham (Ed.) H. Springer handbook of engineering statistics [Internet]. 2006. Available from: http://library1.nida.ac.th/termpaper6/sd/2554/19755.pdf

45. Basalious EB, El-Sebaie W, El-Gazayerly O. Application of pharmaceutical QbD for enhancement of the solubility and dissolution of a class II BCS drug using polymeric surfactants and crystallization inhibitors: development of controlled-release tablets. AAPS PharmSciTech [Internet]. 2011;12:799–810. Available from: https://doi.org/10.1208/s12249-011-9646-6

46. Dawoud MHS, Yassin GE, Ghorab DM, Morsi NM. Insulin mucoadhesive liposomal gel for wound healing: a formulation with sustained release and extended stability using quality by design approach. AAPS PharmSciTech [Internet]. 2019;20:158. Available from: https://doi.org/10.1208/s12249-019-1363-6

47. Khramtsov P, Burdina O, Lazarev S, Novokshonova A, Bochkova M, Timganova V, et al. Modified desolvation method enables simple one-step synthesis of gelatin nanoparticles from different gelatin types with any bloom values. Pharmaceutics. 2021;13:1–26.

48. Migneault I, Catherine D, Michel JB, Karen CW. Glutaraldehyde: behavior in aqueous solution, reaction with proteins, and application to enzyme crosslinking. Biotechniques. 2004;37:790–802.

49. Bhushan B, Dubey P, Kumar SU, Sachdev A, Matai I, Gopinath P. Bionanotherapeutics: niclosamide encapsulated albumin nanoparticles as a novel drug delivery system for cancer therapy. RSC Adv [Internet]. Royal Society of Chemistry. 2015;5:12078–86. Available from: https://doi.org/10.1039/C4RA15233F

50. Lomis N, Westfall S, Farahdel L, Malhotra M, Shum-Tim D, Prakash S. Human serum albumin nanoparticles for use in cancer drug delivery: process optimization and in vitro characterization. Nanomaterials. 2016;6.

51. Dawoud MH., Fayez AM, Mohamed RA, Sweed NM. Optimization of nanovesicular carriers of a poorly soluble drug using factorial design methodology and artificial neural network by applying quality by design approach. Pharm Dev Technol [Internet]. Taylor & Francis. 2021;0:1–50. Available from: https://doi.org/10.1080/10837450.2021.1980009

52. Khadka P, Ro J, Kim H, Kim I, Kim JT, Kim H, et al. Pharmaceutical particle technologies: an approach to improve drug solubility, dissolution and bioavailability. Asian J Pharm Sci [Internet]. Elsevier Ltd. 2014;9:304–16. Available from: https://doi.org/10.1016/j.ajps.2014.05.005

53. Amasya G, Badilli U, Aksu B, Tarimci N. Quality by design case study 1: design of 5-fluorouracil loaded lipid nanoparticles by the W/O/W double emulsion - solvent evaporation method. Eur J Pharm Sci [Internet]. Elsevier BV. 2016;84:92–102. Available from: https://doi.org/10.1016/j.ejps.2016.01.003

54. Noshi SH, Dawoud MHS, Ibrahim MS. A quality by design approach for the optimization of olmesartan medoxomil-orodispersible lyophilisates: in vitro/in vivo evaluation. J Appl Pharm Sci. 2022;12:172–85.

55. Tarhini M, Benlyamani I, Hamdani S, Agusti G, Fessi H, Greige-Gerges H, et al. Protein-based nanoparticle preparation via nanoprecipitation method. Materials (Basel). 2018;11:1–18.

56. Zu Y, Zhang Y, Zhao X, Zhang Q, Liu Y, Jiang R. Optimization of the preparation process of vinblastine sulfate (VBLS)-loaded folate-conjugated bovine serum albumin (BSA) nanoparticles for tumor-targeted drug delivery using response surface methodology (RSM). Int J Nanomedicine. 2009;4:321–33.

57. Jun JY, Nguyen HH, Paik SYR, Chun HS, Kang BC, Ko S. Preparation of size-controlled bovine serum albumin (BSA) nanoparticles by a modified desolvation method. Food Chem [Internet]. Elsevier Ltd. 2011;127:1892–8. Available from: https://doi.org/10.1016/j.foodchem.2011.02.040

58. Ding D, Tang X, Cao X, Wu J, Yuan A, Qiao Q, et al. Novel self-assembly endows human serum albumin nanoparticles with an enhanced antitumor efficacy. AAPS PharmSciTech. 2014;15:213–22.

59. Sadeghi R, Moosavi-Movahedi AA, Emam-Jomeh Z, Kalbasi A, Razavi SH, Karimi M, et al. The effect of different desolvating agents on BSA nanoparticle properties and encapsulation of curcumin. J Nanoparticle Res. 2014;16.

60. Etorki AM, Gao M, Sadeghi R, Maldonado-Mejia LF, Kokini JL. Effects of desolvating agent types, ratios, and temperature on size and nanostructure of nanoparticles from α-lactalbumin and ovalbumin. J Food Sci. 2016;81:E2511–20.

61. Galisteo-González F, Molina-Bolívar JA. Systematic study on the preparation of BSA nanoparticles. Colloids Surfaces B Biointerfaces [Internet]. Elsevier BV. 2014;123:286–92. Available from: https://doi.org/10.1016/j.colsurfb.2014.09.028

62. Fehér B, Lyngsø J, Bartók B, Mihály J, Varga Z, Mészáros R, et al. Effect of pH on the conformation of bovine serume albumin - gold bioconjugates. J Mol Liq [Internet]. Elsevier BV. 2020;309:113065. Available from: https://doi.org/10.1016/j.molliq.2020.113065

63. Sripriyalakshmi S, Anjali CH, George Priya Doss C, Rajith B, Ravindran A. BSA nanoparticle loaded atorvastatin calcium - a new facet for an old drug. PLoS One. 2014;9:1–10.

64. Yoshikawa H, Hirano A, Arakawa T, Shiraki K. Effects of alcohol on the solubility and structure of native and disulfide-modified bovine serum albumin. Int J Biol Macromol [Internet]. Elsevier BV. 2012;50:1286–91. Available from: https://doi.org/10.1016/j.ijbiomac.2012.03.014

65. Bergonzi MC, Guccione C, Grossi C, Piazzini V, Torracchi A, Luccarini I, et al. Albumin nanoparticles for brain delivery: a comparison of chemical versus thermal methods and in vivo behavior. Chem Med Chem. 2016;1840–9.

66. Di Costanzo A, Angelico R. Formulation strategies for enhancing the bioavailability of silymarin: the state of the art. Molecules. 2019;24.

67. Poddar A, Sawant KK. Optimization of galantamine loaded bovine serum albumin nanoparticles by quality by design and its preliminary characterizations. J Nanomed Nanotechnol. 2017;08.

68. Sudhakar B, Krishna MC, Murthy KVR. Factorial design studies of antiretroviral drug-loaded stealth liposomal injectable: PEGylation, lyophilization and pharmacokinetic studies. Appl Nanosci [Internet]. 2016;6:43–60. Available from: https://doi.org/10.1007/s13204-015-0408-8

69. Di Costanzo A, Angelico R. Formulation strategies for enhancing the bioavailability of silymarin: the state of the art. Molecules. 2019;24:1–27.

70. Dhanalakshmi S, Mallikarjuna GU, Singh RP, Agarwal R. Silibinin prevents ultraviolent radiation-caused skin damages in SKH-1 hairless mice via a decrease in thymine dimer positive cells and an up-regulation of p53–p21/Cip1 in epidermis. Carcinogenesis. 2004;25:1459–65.

71. Zi X, Feyes DK, Agarwal R. Anticarcinogenic effect of a flavonoid antioxidant, silymarin, in human breast cancer cells MDA-MB 468: induction of G1 arrest through an increase in Cipl/p21 concomitant with a decrease in kinase activity of cyclin- dependent kinases and associated cycli. Clin Cancer Res. 1998;4:1055–64.

72. Scambia G, De Vincenzo R, Ranelletti FO, Panici PB, Ferrandina G, D'Agostino G, et al. Antiproliferative effect of silybin on gynaecological malignancies: synergism with cisplatin and doxorubicin. Eur J Cancer. 1996;32:877–82.

73. Tyagi AKA, Agarwal C, Singh RP, Shroyer KR, Glode LM, Agarwal R, et al. Silibinin causes cell cycle arrest and apoptosis in human bladder transitional cell carcinoma cells by regulating CDKI-CDK-cyclin cascade, and caspase 3 and PARP cleavages. Carcinogenesis. 2004;25:1711–20.

74. Deep G, Singh RP, Agarwal C, Kroll DJ, Agarwal R. Silymarin and silibinin cause G1 and G2-M cell cycle arrest via distinct circuitries in human prostate cancer PC3 cells: a comparison of flavanone silibinin with flavanolignan mixture silymarin. Oncogene. 2006;25:1053–69.

75. Ramakrishnan G, Lo Muzio L, Elinos-Báez CM, Jagan S, Augustine TA, Kamaraj S, et al. Silymarin inhibited proliferation and induced apoptosis in hepatic cancer cells. Cell Prolif. 2009;42:229–40.

76. Sharma G, Singh RP, Chan DC, Agarwal R. Silibinin induces growth inhibition and apoptotic cell death in human lung carcinoma cells. Anticancer Res [Internet]. Department of Pharmaceutical Sciences, School of Pharmacy, University of Colorado Health Sciences Center, 4200 East 9th Avenue, Box C238, Denver, CO 80262, USA. 2003;23:2649–55. Available from: http://europepmc.org/abstract/MED/12894553